High Density Polyethylene/Micro Calcium Carbonate Composites: A Study of the Morphological, Thermal, and Viscoelastic Properties

Rabeh H. Elleithy,[1] Ilias Ali,[2] Muhammad Alhaj Ali,[2] S. M. Al-Zahrani[2,3]

[1]*SABIC Polymer Research Chair (SPRC), King Saud University, Riyadh 11421, Saudi Arabia*
[2]*Chemical Engineering Department, King Saud University, Riyadh 11421, Saudi Arabia*
[3]*Center of Excellence on Research of Engineering Material (CEREM), King Saud University, Riyadh 11421, Saudi Arabia*

Received 23 October 2009; accepted 13 January 2010
DOI 10.1002/app.32142
Published online 13 April 2010 in Wiley InterScience (www.interscience.wiley.com).

ABSTRACT: High density polyethylene (HDPE) with micro calcium carbonate ($CaCO_3$) masterbatch was pelletized by using a twin screw extruder and different ASTM specimens were molded by an injection molding machine. The morphology of the composites was characterized by scanning electron microscopy (SEM) and Image Analysis software. The dispersion and interfacial interaction between $CaCO_3$ and the polymer matrix were also investigated by SEM. The thermal properties of HDPE and its composites were investigated by differential scanning calorimetry (DSC). The crystallization process of the composites samples was found to be slightly different than that of the neat HDPE. Otherwise, the presence of $CaCO_3$ did not have a considerable effect on the melting behavior of the composites. Thermogravimetric analysis (TGA) revealed that the composites had better thermal stability than the neat HDPE resin as indicated by a higher temperature of 50% weight loss ($T_{50\%}$) for the composites as compared to that of the neat resin. The viscoelastic properties of the composites and HDPE were also investigated via torsional and rotational techniques. The presence of $CaCO_3$ increased the shear modulus at low frequency of the composites at 80°C over that of the neat resin. However, at higher frequencies, the difference between the neat resin and the composites' shear modulus was less than that at low frequencies. The complex viscosity of the composite increased upon the addition of $CaCO_3$. However, the shear sensitivities of the neat resin and the microcomposite were similar. J Appl Polym Sci 117: 2413–2421, 2010

Key words: morphology; thermal; viscoelastic; micro $CaCO_3$; masterbatch; HDPE

INTRODUCTION

Inexpensive inorganic substances are widely used as fillers to improve mechanical and thermal properties of polymers in the plastic industry. These mainly include fillers, such as calcium carbonate ($CaCO_3$), mica, wollastonite, glass fiber, glass beads, jute, silica (SiO_2), etc.[1–3] In recent years micro- and nano-fillers have attracted great interest, both in industry and in academia, because they often exhibit remarkable improvement in materials properties when compared to conventional composites made by using macro-fillers.[4] These micro-/nano-composites can be made with very low loading of micro-/nano-fillers as compared with macro particle sized fillers. Some of these nanocomposites have combined the advantages of the matrix polymer and the unique characteristics of metal nanoparticles.[5–7] High density polyethylene (HDPE) is widely used as a commodity polymer with high-tonnage production due to its distinctive mechanical and physical properties. Because of its low toughness, weather resistance, and environmental stress cracking resistance as compared to engineering polymers, its application in many areas has been limited. To improve these disadvantages, HDPE has been reinforced with fillers.[8–11] HDPE filled with mineral particles also improves dimensional stability, opacity, and barrier properties. $CaCO_3$ is the largest volume mineral used in the polymer industry because of its low cost and abundance. It is available globally in a variety of particle shapes, purities, and sizes (macro, micro, and nano). However, because of its higher polar nature and higher surface areas, $CaCO_3$ is difficult to disperse and stabilize in a polymer matrix. However, $CaCO_3$ could be modified with steric acid to improve dispersion and compatibility with a polymer matrix. Poor dispersion and adhesion of filler leads to a composite with poor final physical

Correspondence to: R. H. Elleithy (rhelleithy@yahoo.com).
Contract grant sponsor: CEREM (King Saud University).

properties.[12–15] Yet, poor adhesion of $CaCO_3$ to the polymer matrix is an beneficial property that was used to enhance the breathability of polymeric films.

The effect of addition of nanosized calcium carbonate with polyethylene on tensile properties, viscosity, and dimensional stability has been investigated by some researchers. Lazzeria et al.[16] fabricated PE nanocomposite with 70% improved Young's modulus compared to virgin PE. The creep behavior of PE nanocomposites reinforced with different nanosized calcium carbonate depends strongly on the calcium carbonate content. One study showed that the best creep resistance of PE nanocomposites can be achieved at 10% of calcium carbonate incorporation in the composite.[17] Low density PE with copper filler, HDPE/montmorillonite, and HDPE/vermiculite have also been reported in the literature and showed improved mechanical performance.[18,19] It has also been demonstrated that the addition of nanoscale fillers influence not only the mechanical properties but also the crystallization.[20] The dispersed nanoscale fillers may act as a heterogeneous nucleation agent to enhance the crystallization rate of the PE matrix, and the fillers, at the same time, may also hinder the transport of the molecule chains to reduce the crystallization growth rate.[20] Zebarjad et al.[14] reported that nanosized calcium carbonate has a significant effect on crystallinity, melting point, and heat of melting of HDPE. Additionally, calcium carbonate could have a significant effect on rheological behavior of HDPE. Moreover, decreasing $CaCO_3$ particle size from micro to nano could affect the barrier properties of the composite. Even though a substantial amount of research has been done on HDPE/$CaCO_3$ composites, the subject still attracts many researchers because of its industrial importance.[21–25] Despite the efforts that have been directed towards the preparation and characterization of polymer micro- and nano-composites, there are questions remaining about their structure, mechanisms of reinforcement, and processing characteristics.[26]

With the current growth in the automotive market, part molders are demanding more processable materials to meet the increasing demand. In addition, in the durable goods sector, parts are also getting thinner and require materials that can be processed more easily. Additionally, from the fabricator's point of view, easy processing and manufacturing of these composites are related directly to productivity. Therefore, the rheological properties of the composites are of vital importance.

In the context of industrial applications, melt blending is the preferred method of composite preparation. Melt blending using masterbatch is one of the simplest, economical, and environmental-friendly methods in processing of plastic composites. Generally, a masterbatch of high concentration of microparticles and a polymer carrier is used as the starting material. Then, the masterbatch is diluted by the pure polymer in a subsequent melt-blending process to get the desired loading of the microparticles in the composite. Masterbatches are often used to improve the uniform distribution of concentrated fillers in the polymer matrix.

Fabrication of composites is mostly done by the incorporation of filler; macro, micro, nano; to the polymer matrix. Micofillers can become airborne during loading into the polymer, which can create an environmental concern; therefore filler incorporation in the polymer matrix needs a special type of arrangement in the extruder. A few reports are available in the literature for the preparation of a composite by masterbatch approach.[27,28] In a masterbatch approach, the dispersion and/or distribution of the microfillers in composite could be controlled by adjusting the processing conditions. Thus the challenge is to fabricate these composite in an industrial scale such that it can meet the demand while having processing advantages for the product manufacturers. Therefore, the masterbatch containing microfillers approach to prepare HDPE composites seems to be attractive and eco friendly.

This study is part of a larger effort to prepare HDPE composite with processing advantages by incorporating the microscale $CaCO_3$ through a masterbatch approach. The masterbatch contained both the polymer carrier and the microfillers. In this study, firstly, the masterbatch was dry blended with the HDPE polymer matrix, them this dry blend was compounded using a twin screw extruder. This article reports the fabrication of HDPE/$CaCO_3$ composite using various loadings of $CaCO_3$. The dispersion and distribution of $CaCO_3$ in the composite was characterized by scanning electron microscope (SEM) and image analysis software. The effect of $CaCO_3$ incorporation on the thermal properties of the composites was investigated by DSC and TGA. Viscoelastic characterization of the matrix polymer and composites were also investigated and reported in this work.

MATERIALS AND METHODS

Materials

High density polyethylene (HDPE-54) from the local market was used in this work. It is an injection molding grade of HDPE copolymer with a narrow molecular weight distribution and high flowability. A list of some of its properties is shown in Table I as provided by the supplier. Micro Filler-0189, a masterbatch containing 80 ± 3% micro $CaCO_3$ was supplied by Wuxi Changhong Masterbatches Co, China. The masterbatch has LLDPE as a carrier for the micro $CaCO_3$. Some of the typical properties of

TABLE I
Physical Properties of HDPE-54 and $CaCO_3$ Masterbatch Used

Physical properties	Unit	Value	ASTM method
HDPE-54, *reported by supplier*			
Melt index	g/10 min	30.0	D-1238
Density	g/cm^3	0.954	D-1505
Vicat softening point	°C	128	D-1525
Tensile strength @ yield	MPa	1200	D-638
Hardness	Shore D	68	D-2240
Brittleness temperature	°C	< -75	D-746
$CaCO_3$ masterbatch, *reported by supplier*			
Granule size for $CaCO_3$	–	20 nm → 2 μm	N/A
Melt flow index (g/10 min)	g/10 min	≤3.0	
Water ratio	%	≤0.15	
Carrier	LLDPE		
Melt temperature	°C	125	
Health and safety	Confirms with European Resolution AP 89(1)		

the masterbatch used are listed in Table I as listed in the supplier datasheet. Please note that the surface of $CaCO_3$ is not treated. Using untreated $CaCO_3$ is economical and it will enhance debonding of the micro particles, which in turn enhances the permeability of the composite that finds applications in the breathable films, as indicated by the manufacturer.

Compounding

HDPE was dry blended with different $CaCO_3$ masterbatch ratios, namely 10 and 20%. The dry blend was pelletized using an intermeshing and corotating twin screw extruder, Farrell FTX20. The screw diameter was 26 mm and the length to diameter ratio was 35. The screw had both dispersive and distributive mixing elements. The dry blends were fed to the extruder, which was operating at a screw speed of 12 rpm and at average processing temperature of 235°C. The melt pressure was about 7 bar. The extrudate was cooled in a water bath, dried, and pelletized for further use. The details of the compounding conditions are listed in Table II. One control material, NC-0, and two different composites; NC-10, NC-20, were prepared as listed in Table III and ASTM specimens were molded for further testing.

Injection molding

An Injection Molding Machine (Asian Plastic Machinery Co., Double Toggle IM Machine, Super Master Series SM 120) was used to mold samples for further testing. The molding conditions are listed in Table II. The molded specimens were conditioned at 23°C for 24 h before testing.

Morphological analysis

A small quantity of the masterbatch was placed in a muffle furnace and heated to more than 800°C to ash the LLDPE present in the masterbatch and recover the $CaCO_3$. These steps are similar to the pyrolysis process. The $CaCO_3$ so obtained was deagglomerated by mortar and pestle and used for SEM (JSM 6360A, JEOL), analysis. Furthermore, the SEM was used to observe the surface morphology of the as-molded specimens as well as the cryofractured samples. The cryofractured samples were prepared by soaking molded samples, which contain a controlled crack in liquid nitrogen for more than 5 min, then quickly fracture them using impact force to avoid material deformation. The surfaces of the samples were coated with gold under vacuum before the SEM observation to avoid electrostatic charging during examination. Furthermore, the cryofractured surface was analyzed using image analysis software by SigmaPlot.

Differential scanning calorimetry

Differential scanning calorimetry (DSC) Shimadzu DSC-60 was used for this analysis. Specimens of about 6–7 mg each were prepared out of the compounded pellets. Each specimen was prepared by ''shaving-off'' a thin layer, less than 1 mm thickness, of the pellets to minimize the thickness effect. Each specimen was put in an aluminum pan without being sealed then placed in the DSC oven in air at atmospheric pressure. Samples were heated at 5°C/min from room temperature to 200°C, held at this temperature for 10 min, and then cooled back to room temperature at a cooling rate of 5°C/min. The melting temperature (T_m) and the crystallization temperature (T_c) of HDPE were taken at the peaks of the melting and crystallization processes, respectively. The onset crystallization temperature (T_{oc})

TABLE II
Details of Extrusion and Injection Molding Conditions

Extrusion condition					
Zone - V	Zone - IV	Zone - IV	Zone - III	Zone - II	Feed zone
235	240	240	235	230	180

Injection molding conditions					
Temperature profile (°C)				Cool time (sec)	Water circulation temperature (°C)
Die Zone	Zone III	Zone II	Feed Zone	15	10-11
210	230	220	160		

was determined at the beginning of the crystallization (at the intersection of the peak slope with the baseline). The melting and crystallization enthalpies, (ΔH_m) and (ΔH_c), were determined from the corresponding peak areas in the heating and cooling DSC scans, respectively.

Thermogravimetric analysis

Thermogravimetric analysis (TGA) was performed using a PerkinElmer TGA-7 thermogravimetric analyzer. Samples weighing about 10 mg each were heated up to 600°C in air with a heating rate of 20°C/min. The decomposition temperature $T_{50\%}$ was used to judge the decomposition of the material. The decomposition temperature $T_{50\%}$ is defined as the temperature at which the material has lost 50% of its original weight.

Viscoelastic properties

The viscoelastic properties of the samples were characterized with AR G2 Rheometer made by TA. The linear viscoelastic storage and loss moduli were measured in torsion mode at 80°C. The limits for the rotation angular frequency varying between 0.1 to 100 rad/s. The specimen for this analysis was taken from injection molded samples cut into rectangular stripes of 28 × 3.20 × 13.4 mm^3 to fit the rheometer's fixtures. The temperature was stable within 0.2°C over the range used in this study. The torsion moduli reported in the following are those measured in the linear viscoelastic response region. All tests were performed in air atmosphere.

For the dynamic linear viscoelasticity of the melt, the samples were compression-molded at 190°C under a pressure with required diameter disks to fit the rheometer fixtures. The linear viscoelastic functions were measured using the parallel plate geometry (diameter = 25 mm and gap = 1000 micron). Frequency scans were performed in the range between 0.1 to 100 rad/s at 190°C. Strain sweeps were previously performed to investigate the linear viscoelastic response region, and time sweeps were also performed to test the melt stability of the samples.

All of the reported measurements for all of the experiments are the representation of three different experiments.

RESULTS AND DISCUSSION

Morphological analysis

As the filler size, shape, and loading directly affect the performance of composite, Figure 1(a) shows the SEM images of $CaCO_3$ obtained after ashing of the masterbatch as describe previously. The SEM micrograph in Figure 1(a) shows the agglomeration of $CaCO_3$. It is known that $CaCO_3$ has a great tendency to form agglomerates, in fact, agglomeration is a well-known phenomenon, and its probability increases with decreasing particle size.[29] The occurrence and extent of agglomeration are determined by the relative magnitude of the forces, which either bind together the particles or try to separate them. Hornsby listed mechanical interlocking, electrostatic forces, van der Waals forces, and liquid and solid bridging as the principle adhesive forces between particles.[30,31] All of these factors could have participated in the agglomeration of the $CaCO_3$ particles seen in Figure 1(a).

The surface morphologies of NC-10 and NC-20 are depicted in the SEM micrograph of Figure 1(b). A reasonably good distribution of $CaCO_3$ was achieved in the composite; however, agglomeration of $CaCO_3$ was still observed. This agglomeration is a sign of low dispersion that was mainly caused by the tendency of $CaCO_3$ particles to agglomerate as mentioned earlier.

The SEM micrographs of cryofractured NC-10 and NC-20 are shown in Figure 1(c). A reasonably even distribution of $CaCO_3$ in the matrix of the composite was observed. It is evident that the $CaCO_3$ present

TABLE III
A List of the Samples Prepared for this Work

Sample	Description
NC-0	HDPE-54 + 0% $CaCO_3$ filler masterbatch
NC-10	HDPE-54 + 10% $CaCO_3$ filler masterbatch
NC-20	HDPE-54 + 20% $CaCO_3$ filler masterbatch

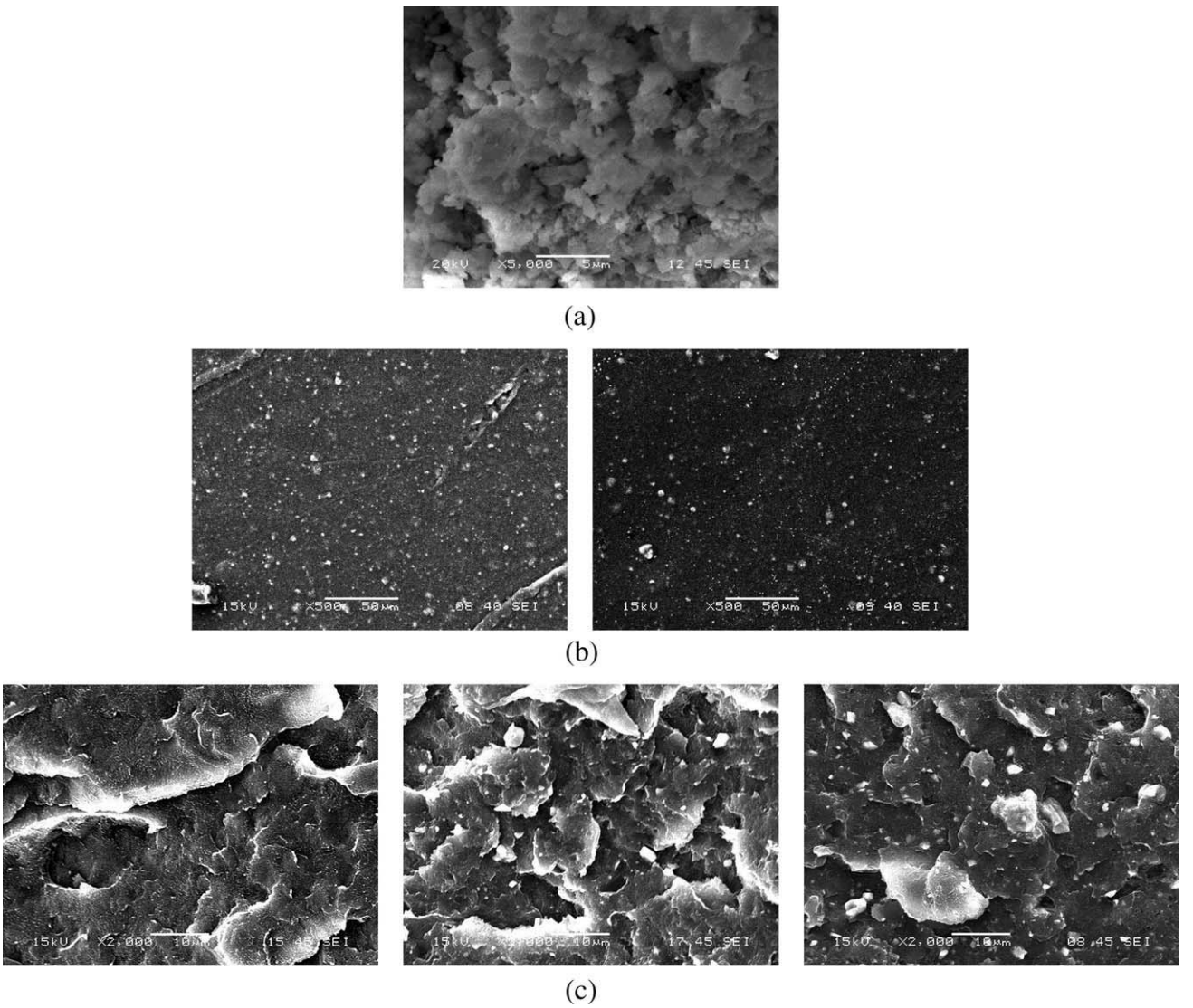

Figure 1 SEM micrographs of (a) $CaCO_3$ obtained from masterbatch, (b) surfaces of NC-10 and NC-20, and (c) surfaces of NC-0, NC-10, and NC-20.

still had some level of aggregation in the composite sample similar to $CaCO_3$ present in the masterbatch as seen in Figure 1(a) and in the surface of Figure 1(b). The microparticles tend to decrease their surface contact with the matrix by agglomeration, and these microparticle aggregates could act like a single big particle as seen in Figure 1(c). These agglomerated particles could be stress concentrator points and could affect the final performance of the composite. The details of the mechanical properties of these composites are the subject of our current investigation and will be submitted for publication shortly.

The distribution of the micro $CaCO_3$ particles is shown in Figure 2. Keep in mind that this distribution cover microparticles with area bigger than 1 micron only. Smaller particles were not analyzed here due to the limitations of the used SEM. It is observed that the highest population of the particles has an area under 5 μm^2. Additionally, most of the particles were under 10 μm^2. It is also noticed that NC-10 had more smaller particles than NC-20. This could indicate that the dispersion efficiency decreased as the micro $CaCO_3$ percentage increased.

Thermal properties

DSC analysis

Figure 3(a) depicts the dynamic temperature thermograms of NC-0, NC-10, and NC-20 composites. The thermograms were shifted vertically for ease of presentation. The endothermic melting peaks for all materials looked similar; however, two differences in the melting behavior between NC-0 and NC-10 or NC-20 could be observed. Firstly, the melting temperature (T_m) increased slightly for NC-10 and NC-

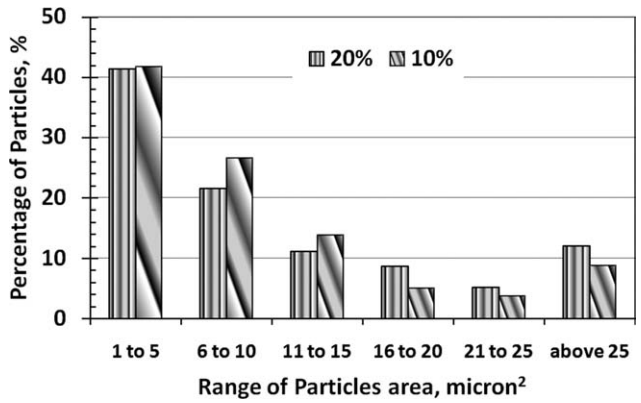

Figure 2 Calcium carbonate particle size distribution for particles bigger than 1 micron for NC-10 and NC-20 micro-composites.

20 composite samples as illustrated in Table IV. Higher melting temperatures are indicative of thicker lamella as indicated by the Thompson-Gibbs equation.[13] Such thickness-melting dependence of PE crystallites is well documented in literature.[13,32] Secondly; the relative crystallinity (X_r) decreased as the percentage of $CaCO_3$ increased as shown in Table IV. The relative crystallinity (X_r) was calculated using the eq. (1).

$$X_r = \Delta H_{\text{Composite}}/\Delta H_{\text{Neat resin}} \quad (1)$$

The enthalpy of the composite or the neat resin is ΔH. The incorporation of the $CaCO_3$ in the composites samples lowers the enthalpy of NC-10 and NC-20 as compared NC-0. The reduction of the enthalpy of NC-10 and NC-20 means that the needed heat to melt the polymer is reduced, which is translated to power and money savings during extrusion or molding processes. The reduction of the composite enthalpy and crystallinity could be explained by the reduction of the conformational changes available to the macromolecules during crystallization, which is due to the presence of the $CaCO_3$ in the composite. Calcium Carbonate restricts the macromolecular mobility and reduces the spaces available to be occupied by the macromolecules according to statistical thermodynamics.[33] The reduction of the conformational changes available to the macromolecules during crystallization was estimated from the reduction

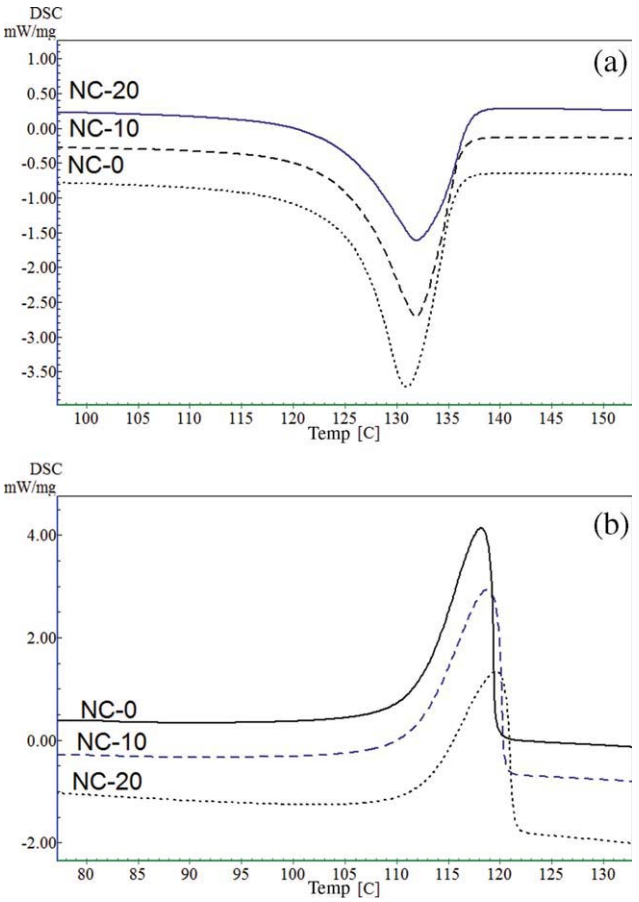

Figure 3 DSC (a) heating and (b) cooling scans of NC-0, NC-10, and NC-20. [Color figure can be viewed in the online issue, which is available at www.interscience.wiley.com.]

of the entropy of crystallization (ΔS_c) as calculated from eq. (2).

$$\Delta S_c = \Delta H_c/T_c \quad (2)$$

Where, ΔH_c is the enthalpy of crystallization, and T_c is the crystallization temperature. As seen from Table IV, the ΔS_c decreased as the percentage of $CaCo_3$ increased. The reduction of ΔS_c is correspondent to the reduction of the freedom available to the macromolecule.

Figure 3(b) shows the cooling thermograms of NC-0, NC-10, and NC-20. The shapes of the exothermic crystallization peak of all the samples were comparable to each other. However, some differences

TABLE IV
Thermodynamic Properties of NC-0, NC-10, and NC-20

Sample	T_m (°C)	X_r	ΔS_c (j/g, °C)	ΔT (°C)
NC-0	130.9 ± 0.5	1.00	2.43 ± 0.1	12.8 ± 1.0
NC-10	131.9 ± 0.5	0.89 ± 0.6	2.16 ± 0.1	13.1 ± 1.0
NC-20	131.3 ± 0.5	0.87 ± 0.6	1.86 ± 0.1	12.0 ± 1.0

TABLE V
TGA Analysis of NC-0, NC-10, and NC-20

Sample	$T_{50\%}$ (°C)
NC-0	420 ± 3
NC-10	432 ± 3
NC-20	456 ± 3

were observed as seen from Table IV. In a programmed cooling, the crystallization temperature (T_c) or the degree of supercooling (ΔT) reflect the overall crystallization rate attributed to the combined effects of nucleation and growth. The degree of supercooling (ΔT) is calculated from eq. (3).

$$\Delta T = T_m - T_c \tag{3}$$

The ΔT may be considered as a measurement of polymer's crystallizability, so the smaller the ΔT, the higher the overall crystallization rate.[34] The ΔT value for the NC-20 composite is smaller than that of NC-0 or NC-10 as seen from Table IV. Therefore, the overall crystallization rate of composites NC-20 would be higher than of NC-0 or NC-10. However, the difference in ΔT is small, thus the expected differences in the crystallization rates would be small as well, as seen in Figure 3(b).

TGA analysis

As seen from Table V a**nd** Figure 4, $T_{50\%}$ increased as the percentage of $CaCO_3$ increased. This increase in $T_{50\%}$ could be due to more than a single factor. One factor is the high thermal resistance of the micro $CaCO_3$, which has an onset degradation temperature of about 550°C.[35] Another factor could be the contribution of $CaCO_3$ in minimizing the permeation of the heat into the HDPE matrix.[36] Not only did $T_{50\%}$ increase for NC-10 and NC-20, but also the onset degradation temperature increased as well, as seen from Figure 4. Additionally, the decomposition rate decreased as the percentage of micro $CaCO_3$ increased, as depicted in Figure 4 as well. All of these observations indicated that the thermal resistance of NC-10 and NC-20 increased by the incorporation of the micro $CaCO_3$ into the composite.

For verification purposes, the molar thermal decomposition function $Y_{d,1/2}$ for polyethylene was calculated from eq. (4).[37]

$$Y_{d,1/2} \approx T_{50\%} \times M \tag{4}$$

Where, M is the molecular weight per repeat unit of the polymer. Our calculations indicated that $Y_{d,1/2}$ is equal to 19.4, whereas, the reported value by Bicerano was 19.0.[37] The agreement between the two values is obvious.

Viscoelastic properties

Solid state

The storage moduli (G') of NC-0, NC-10, and NC-20 at 80°C are plotted against the radial frequency in Figure 5. Compared to NC-0, the storage moduli (G') of NC-10 and NC-20 slightly increased, especially at low frequency. However, at high frequencies, G' of all materials were very close to each other as seen in Figure 5. These results suggest that NC-10 and NC-20 could have higher creep moduli than that of NC-0; however, the moduli of all materials under impact would be the same. The storage modulus enhancement could be attributed to stiffness imparted by $CaCO_3$ microparticles, which will increase the overall stiffness of the composites as compared to the neat resin. In the low frequency range, the composite behavior deviated from that of neat HDPE, which

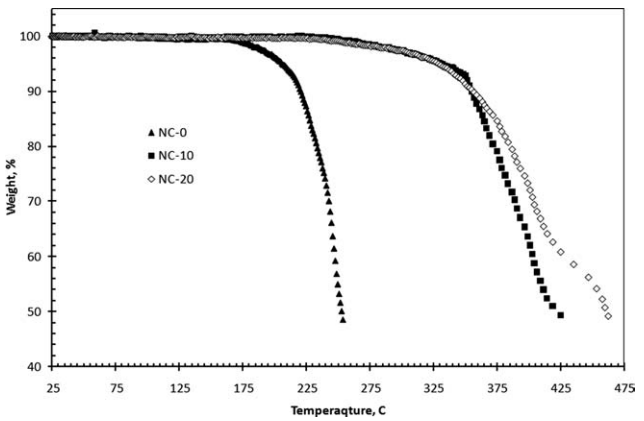

Figure 4 TGA thermograms of NC-0 and composite sample NC-10 and NC-20.

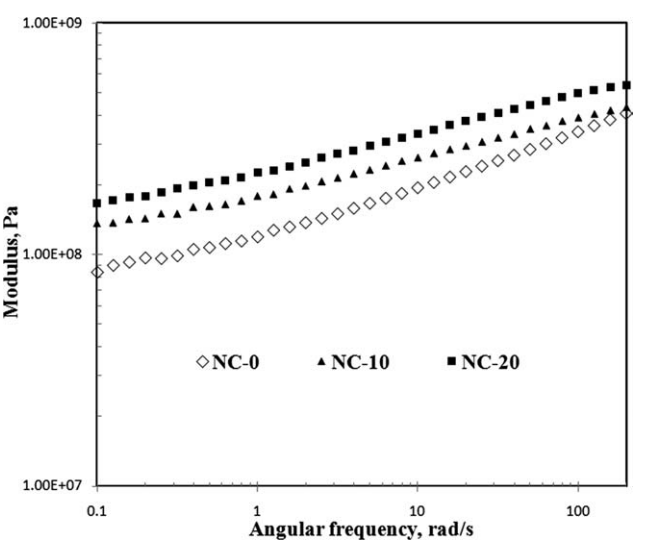

Figure 5 Dynamic modulus curve of NC-0, NC-10, and NC-20 at 80°C.

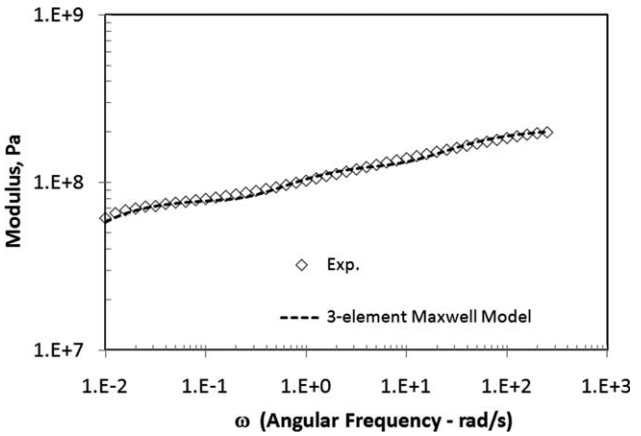

Figure 6 Experimental and three-element Maxwell model fit for NC-20.

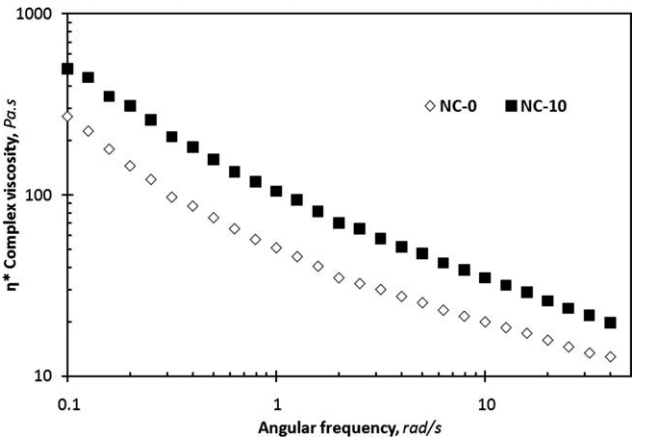

Figure 7 η* vs. ω curves of NC-0 and NC-10 at 190°C.

could be due to the increased heterogeneity of the composites due to the presence of the $CaCO_3$ particles.[36] However, the overall behavior of G' versus G'' of all materials was similar to each other, which shows that the molecular mobility of the composites and the neat resin are analogous to each other. This would suggest that there is a limited interaction between the matrix and the $CaCO_3$ particles, which was confirmed by the morphological analysis.

The relationship of the complex modulus (G^*) versus the angular frequency (ω) is modeled using the three-element Maxwell model, which has the following general form.[38]

$$G(t) = G_1 e^{-t/\tau_1} + G_2 e^{-t/\tau_2} + G_3 e^{-t/\tau_3} \quad (5)$$

Where $G(t)$ is the shear modulus of the material, G_i and τ_i are constants to be determined from the fitting of the model to the experimental data. The model and the experimental data are shown in Figure 6 for NC-20. The values of G_i and τ_i for NC-0 and the composites are shown in Table VI. The constants G_1 and τ_1 affect the low frequency behavior; whereas, the constants G_3 and τ_3 affect more the high frequency response. It is noticed that the values of τ_i for the composites are higher than those of the neat resin, which is an indication that the relaxation time of the composites is longer than that of the resin. Longer relaxation time would suggest more extrudate swell during extrusion.

TABLE VI
The Constants for a Three Element Maxwell Model for NC-0, NC-10, and NC-20

	G_1	G_2	G_3	τ_1	τ_2	τ_3
NC-0	7.01E07	6.14E07	5.16E07	279	0.03	0.79
NC-10	7.51E07	6.14E07	5.16E07	313	0.03	1.24
NC-20	8.01E07	7.67E07	5.16E7	313	0.04	1.39

Melt state

A plot of the complex viscosity, η*, versus the angular frequency, ω, for NC-0 and NC-10 at 190°C are shown in Figure 7. Both materials had similar shear sensitivity as indicated by the similar slope of η* versus ω. However, η* of NC-10 was higher than that of NC-0, which may be due to the presence of $CaCO_3$ microparticles. The microparticles would have disturbed the normal flow of polymer and increased its viscosity. This phenomenon is usually observed in dilute suspensions of rigid particles.[39,40]

CONCLUSIONS

HDPE/micro $CaCO_3$ composites were effectively melt blended from masterbatch by using a twin screw extruder, then injection molded samples were successfully prepared. The morphological analysis revealed that the $CaCO_3$ had some agglomeration but was reasonably distributed across the injection molded samples. The presence of $CaCO_3$ influenced the crystallization of HDPE by reducing the crystallinity and the entropy of crystallization of the composites. TGA analysis of the composite samples showed that the thermal stability of the composites increased as indicated by the increase of the onset degradation temperature and $T_{50\%}$. The G' and G^* of NC-10 and NC-20 increased as compared to NC-0, especially at low frequencies. A three-element model was used successfully to describe the viscoelastic behavior of the materials, which indicated the increase of the relaxation time of the composites as compared to the neat resin. The addition of $CaCo_3$ microparticles did not affect the shear sensitivity of the composite, but it increased its viscosity as compared to the neat resin.

Authors would like to thank SABIC Polymer Research Chair at King Saud University for providing their equipment to conduct these tests. Special thanks to Mujtahid, Sarwono,

Babu, Achmad, and Imtiaz for conducting some of the experimental work in this research.

References

1. Bhattachrya, S.; Gupta, R.; Kamal, M. R. Polymeric Nanocomposite: Theory and Practice; Hanser: Munich, Germany, 2007; Chapter 1.
2. Nguyen, H. X.; Ishida, H. Polym Compos 1987, 8, 57.
3. Menendez, H.; White, J. L. Polym Eng Sci 1984, 24, 1051.
4. Ray, S. S.; Okamoto, M. Prog Polym Sci 2003, 28, 1539.
5. Tjong, S. C.; Bao, S. P. J Polym Sci Part B: Polym Phys 2005, 43, 253.
6. Liu, X.; Wu, Q.; Berglund, L. A.; Qi, Z. N. Macromol Mater Eng 2002, 287, 515.
7. Wu, T. M.; Hsu, S. F.; Wu, J. Y. J Polym Sci Part B: Polym Phys 2003, 41, 560.
8. Wang, Y.; Shi, J.; Han, L.; Xiang, F. Mater Sci Eng A 2009, 501, 220.
9. Rothon, R. N. Particulate-Filled Polymer Composites; Longman Scientific and Technical: Harlow, 1995.
10. Rothon, R. N. Adv Polym Sci 1999, 139, 67.
11. Argon, A. S.; Bartczak, Z.; Cohen, R. E.; Muratoglu, O. K. Toughening of Plastics, Advances in Modeling and Experiments, Symposium Series 759; Pearson, R. A., Sue, H. J., Yee, A. F., Eds.; ACS: Washington, DC, 2000; p 98.
12. Jingxin, L.; Rong, Z. Polym Eng Sci 2000, 40, 1529.
13. Sahebiana, S.; Zebarjada, S. M.; Khakia, J. V.; Sajjadi, S. A. J Mater Process Technol 2009, 209, 1310.
14. Zebarjad, S. M.; Sajjadi, S. A. Mater Sci Eng A 2008, 475, 365.
15. Tingxiu, X.; Hongzhi, L.; Yuchun, O.; Guisheng, Y. J Polym Sci Part B: Polym Phys 2005, 43, 3213.
16. Lazzeria, A.; Zebarjadb, S. M.; Pracellac, M.; Cavalierd, K.; Rosam, R. Polymer 2005, 46, 827.
17. Sahebian, S.; Sherafat, Z.; Zebarjad, S. M.; Sajjadi, S. A. Presented at the 9th Annual Meeting of Iranian Society of Metallurgical Engineers, Shiraz, Iran, November 15–16, 2005.
18. Xia, X.; Xie, C.; Cai, S. Thermochim Acta 2005, 427, 129.
19. Liang, G.; Xu, J.; Xu, W. J Appl Polym Sci 2004, 91, 3054.
20. Huang, J. W.; Wen, Y. L.; Kang, C. C.; Tseng, W. J.; Ye, M. Y. Polym Eng Sci 2008, 48, 1268.
21. Kaully, T.; Siegmann, A.; Shacham, D. Polym Adv Technol 2007, 18, 696.
22. Papirer, E.; Schultz, J.; Turchi, C. Euro Polym J 1984, 12, 1155.
23. Li, L.; White, J. L. Rubber Chem Technol 1996, 69, 628.
24. Yu, D.; Wu, Q.; Ren, Z. Presented at the XIIIth International Congress on Rheology; Cambridge, UK, 2000.
25. Shenoy, A. V. Rheology of Filled Polymer Systems; Kluwer Academic Publishers: London, 1999.
26. Kelarakis, A.; Yoon, K.; Sics, I.; Somani, R. H.; Hsiao, B. S.; Chu, B. Polymer 2005, 46, 5103.
27. Lee, S. H.; Kim, M. W.; Kim, S. H.; You, J. R. Euro Polym J 2008, 44, 1620.
28. Potschke, P.; Fornes, T. D.; Paul, D. R. Polymer 2002, 43, 3247.
29. Sahebian, S.; Zebarjad, S. M.; Sajjadi, S. A.; Sherafat, Z.; Lazzeri, A. J Appl Polym Sci 2007, 104, 3688.
30. Hornsby, P. R.; Premphet, K. J. J Appl Polym Sci 1998, 70, 587.
31. Hornsby, P. R. In Rheology, compounding and processing of filled thermoplastics. Mineral fillers in thermoplastics-I raw materials and processing; Jancar, J., Ed.; Advances in Polymer Science; Springer-Verlag: New York, 1999; Vol 139, p 155.
32. Wunderlichm, B. Macromolecular Physics; Academic press: New York, 1973; Vol 3.
33. Sperling, L. H. In Introduction to Physical Polymer Science, 2nd ed.; Wiley Interscience: New York, 1992.
34. Cheng, F.; Mong, T.; Jia, R. L. J Polym Res 2003, 10, 127.
35. Zweifel, H. Plastic Additives Handbook, 5th ed.; Hanser: Munich, Germany, 2001.
36. Chae, D. W.; Kim, K. J.; Kim, B. C. Polymer 2006, 47, 3609.
37. Bicerano, J. Prediction of Polymer Properties; Marcel Dekker Inc: New York, 1993.
38. Ferry, J. Viscoelastic Properties of Polymers, 3rd ed.; John Wiley & Sons: New York, 1980.
39. Solomon, M. J.; Almusallam, A. S.; Seefeldt, K. F.; Somwangthanaroj, A.; Varadan, P. Macromolecules 2001, 34, 1864.
40. Huang, Y. Q.; Zhang, Y. Q.; Hua, Y. Q. J Mater Sci Lett 2003, 22, 997.